Baroclinic Instability of the Summer Mesosphere: A Mechanism for the Quasi-Two-Day Wave?

R. ALAN PLUMB

CSIRO Division of Atmospheric Physics, Aspendale 3195, Australia

(Manuscript received 28 July 1981, in final form 25 August 1982)

ABSTRACT

Observations of the "quasi-two-day" wave are reviewed and it is concluded that the weight of evidence indicates that the wave is a solstical phenomenon, with maximum amplitudes in low latitudes of the summer mesosphere. It is suggested that the properties of this wave and of a similar wave found in a numerical model of the middle atmosphere may be consistent with an origin via baroclinic instability of the easterly jet in the summer mesosphere. This suggestion is supported by the results of a stability analysis of a one-dimensional model of the summer mesospheric flow.

1. The "two-day" wave

Over the past 15 years or so compelling evidence has accumulated for the existence of a periodicity of approximately two days in the wind and temperature structure of the upper stratosphere, mesosphere and lower thermosphere. This "two-day-wave" has large amplitude in summer when it has been clearly identified in meteor and partial reflection radar observations of winds above about 80 km (Muller, 1972; Kal'chenko and Bulgakov, 1973; Glass *et al.*, 1975; Kingsley *et al.*, 1978; Muller and Nelson, 1978; Aso *et al.*, 1980; Craig *et al.*, 1980; Salby and Roper, 1980; Craig and Elford, 1981), in rocket observations of winds near the equatorial stratopause (Coy, 1979) and in satellite radiance measurements of the upper stratosphere and mesosphere (Rodgers and Prata, 1981). These recent satellite observations give a clear global picture of the wave structure. In the zonal direction the wave has wavenumber 3 (Rodgers and Prata, 1981), a result consistent with analysis of phase lags of the wind oscillation between radar sites at different longitudes (Glass *et al.*, 1975; Muller and Nelson, 1978; Craig *et al.*, 1980). In latitude, the amplitude of the temperature oscillation maximizes at about 20° in the summer hemisphere and its distribution appears to have a latitudinal scale of some 30–40°. The radar observations seem to imply a similar structure for the meridional wind component, although the penetration to high latitudes may be more pronounced (cf. Kal'chenko and Bulgakov, 1973; Muller and Nelson, 1978; Aso *et al.*, 1980; Cevaloni *et al.*, 1981; Craig and Elford, 1981). The zonal wind component is weak at low latitudes of the summer hemisphere but may be as large as, or slightly greater than, the meridional component at higher latitudes. Typical amplitudes of the zonal wind oscillation at 80–100 km altitude are about 7 m s^{-1} at the equator (Kal'chenko and Bulgakov, 1973), increasing to about 20 m s^{-1} at around 50°N in July/August (Muller and Nelson, 1978). The meridional component is typically 20–25 m s^{-1} in July/August between the equator and about 55°N (Kal'chenko and Bulgakov, 1973; Muller and Nelson, 1978; Aso *et al.*, 1980). The amplitudes seem to be larger in the Southern Hemisphere during January/February, by a factor of about 2; observations at Adelaide (35°S) give typical meridional wind amplitudes of about 50 m s^{-1} (Craig and Elford, 1981) and a similar interhemispheric difference in temperature amplitudes is apparent in the satellite data (Rodgers and Prata, 1981).

In the vertical, satellite observations at around 45, 62 and 85 km show greatest temperature amplitude at 62 km with that at 45 km being smaller by a factor of about 3, suggesting maximum amplitudes in the mesosphere. The wind amplitudes seem to be fairly constant with height at meteor heights (Craig and Elford, 1981). The only observation at lower levels—the rocket data for January 1977 analysed by Coy (1979)—show substantial amplitudes (~20 m s^{-1}) of the meridional wind in the equatorial upper stratosphere, decreasing rapidly below; for comparison, Kal'chenko (1979) reports amplitudes of 35 m s^{-1} at meteor heights during January 1970. There is little evidence of the wave below about 40 km. Stening *et al.* (1978) claimed a correlation between the meteor wind oscillation at Saskatoon and 50 mb temperature at Edmonton, but noted that no clear correlation could be found with 50 mb temperatures at other Canadian stations. Muller (1972) and Muller and Kingsley (1974) noted an apparent correlation between meteor winds and sea level pressure fluctua-

tions. However, the quasi-two-day signal at sea level was associated with the passage of synoptic-scale depressions over the British Isles whereas, as noted above, the meteor wind oscillation is now recognized as being of planetary scale. In view of this fact and of the short data record used, and in the absence of any confirmation from later analyses or at other locations, it seems that this correlation must now be discounted.

In addition to amplitude differences, another apparent difference between the hemispheres in their respective summers is the wave period. In northern summer the wave period seems consistently to be fairly close to 51 h (Muller, 1972; Glass *et al.*, 1975; Muller and Nelson, 1978; Salby and Roper, 1980) whereas in southern summer the period seems to be 48–49 h (Craig *et al.*, 1980; Craig and Elford, 1981). While it is not possible to define the observed period very precisely, if only because of the length of the data records, this difference appears to be real. For example, in the Adelaide time series for January/February 1980 (Fig. 1 of Craig *et al.*, 1980) the wind reversal maintains a fairly constant phase with respect to odd/even dates over the 12 cycles of the record; this could not be maintained over more than four cycles if the period were as long as 51 h.

A fairly consistent picture of the seasonal variability of the wave is emerging. As noted earlier, maximum amplitudes are observed in summer. The variation of amplitude over the year has been determined for meteor winds in the Northern (Kingsley *et al.*, 1978) and Southern (Craig and Elford, 1981) Hemispheres and for both hemispheres in satellite radiance observations (Rodgers and Prata, 1981). These show strong amplification for an interval of about two months centered shortly after summer solstice and a weaker amplification for a comparable period near winter solstice; at other times of the year the amplitude falls to a level that appears indistinguishable from the noise (Prata and Rogers, 1981). Only during the solstice seasons, then, is there clear evidence for a coherent two-day wave. The one observational study that contradicts this statement is that of Salby and Roper (1980) who, analyzing the probability density of certain events in Atlanta meteor wind data as a function of period, found a well-defined isolation of probability at 2.1 days throughout the year. Further, their observed amplitudes [as measured by a (u, v) correlation] maximized in autumn with *minimum* values in summer, in conflict with the other observations cited above.

These latter results excepted, a coherent picture of the spatial and seasonal structure of the wave emerges, *viz.*, of a wavenumber 3 planetary wave, present near solstice, with maximum meridional wind and temperature amplitude in low latitudes of the summer hemisphere, extending with weaker amplitude to higher latitudes and into the winter hemisphere. The vertical structure is not so well established, but the satellite data suggest maximum amplitudes in the mesosphere.

A similar wave has been found in a general circulation model of the middle atmosphere January circulation (Hunt, 1981a,b). Hunt's model has 54 levels (vertical resolution of 2.5 km above 30 km) and has a realistic easterly wind maximum in the summer mesosphere; the model has no diurnal cycle. A prominent feature of the motions in middle and low latitudes of the summer mesosphere is a wave of wavenumber 3 and period a little more than two days (Hunt 1981b). The wave is barotropic except in the region of jet maximum (about 70 km) where there is a substantial baroclinic phase change. This is borne out by the meridional eddy heat flux in this region which exhibits a narrow region of intense equatorward heat flux just below jet maximum and a weaker region of poleward flux above (B. G. Hunt, private communication, 1981). This property may give some clue as to the origin of the wave, as will be discussed below.

2. Theoretical considerations

One interpretation put forward to explain the existence of the wave is that it is an atmospheric normal mode (Salby and Roper, 1980; Salby, 1981). For realistic atmospheric structures, the Rossby-gravity mode of wavenumber 3 has a period of about 2.2 days (Salby, 1981); its amplitude may grow strongly with height in the summer mesosphere where its Doppler-shifted frequency becomes small. Salby's (1981) results thus show large amplitudes in the summer mesosphere but weak mesospheric amplitudes at the equinoxes, in agreement with observation.

Hunt's GCM results, however, suggest an alternative explanation may be necessary. The eddy heat fluxes may be interpreted in terms of the Eliassen-Palm (EP) flux of wave activity (e.g., Edmon *et al.*, 1980) whose vertical component is, for quasi-geostrophic flow,

$$F_z = \rho f \frac{\overline{v'\theta'}}{\partial\bar{\theta}/\partial z}, \tag{1}$$

where ρ is density, f the Coriolis parameter, v northward velocity, θ potential temperature and z height, and where the overbar denotes zonal average and the prime a deviation from that average. Therefore, the heat fluxes can be interpreted as an upward vertical component of the EP flux (equivalent to phase leading with increasing height) above the jet and downward (phase lags with height) below. Analyses of phase leading with height in the meteor wind records (Craig and Elford, 1981) are consistent with this but there is little information to confirm or deny the inferred phase structure below jet maximum apart from the statement of Rodgers and Prata (1981) that the

satellite data show little change of phase between the channels centered on 45 and 62 km.

While it is not possible to be categorical—especially in the presence of nonconservative effects—the implication of divergence of the vertical component of the EP flux in the region of jet maximum seems difficult to reconcile with a normal mode interpretation. In particular Salby's (1981) solstice calculations show increasing phase with height (upward EP flux) throughout the mesosphere equatorward of jet maximum; poleward of jet maximum the phase decreases with height above the level of jet maximum and increases below, a profile that corresponds to a *convergence* of the EP flux. Therefore the normal mode structure appears to be inconsistent with the structure of the wave in Hunt's (1981a,b) model in this very important respect.

This heat flux structure is, however, a characteristic signature of baroclinic instability of internal jets (e.g., McIntyre, 1972; Dickinson, 1973) in which case the concomitant EP flux divergence is indicative of the local generation of wave activity. The EP flux divergence is related to the northward flux of quasi-geostrophic potential vorticity q (Edmon *et al.*, 1980)

$$\nabla \cdot \mathbf{F} = \rho \overline{v'q'}. \tag{2}$$

For conservative motion, $dq/dt = 0$ and hence if the perturbation is linear $q' = -\eta \partial \bar{q}/\partial y$, where η is the northward particle displacement from its unperturbed latitude such that $v' = (\partial/\partial t + \bar{u}\partial/\partial x)\eta$ and y is the northward coordinate. Then (2) may be written

$$\nabla \cdot \mathbf{F} = -\frac{\partial}{\partial t}\left(\frac{1}{2}\overline{\eta}^2\right)\rho \frac{\partial \bar{q}}{\partial y}. \tag{3}$$

Instability may be possible if $\partial \bar{q}/\partial y$ changes sign somewhere (Charney and Stern, 1962). For an unstable internal jet in the atmosphere, $\partial \bar{q}/\partial y$ will be negative in a confined region and positive elsewhere. For a growing disturbance, $\partial(\frac{1}{2}\overline{\eta}^2)/\partial t > 0$ and (3) therefore states that **F** will be divergent in this region of negative potential vorticity gradient and convergent elsewhere, a pattern which, superficially at least, is consistent with Hunt's results.

That the easterly jet of the summer mesosphere might be unstable was suggested by Dickinson (1973) and actual solutions for some idealized profiles were obtained by Simmons (1977). Simmons found that growing modes propagate only weakly relative to the jet and found the most rapidly growing modes to have zonal wavelengths of 4000–6000 km and periods of about 1 day. Most of Simmons' profiles comprised an easterly jet at or just above the stratopause; "climatological" profiles given by Murgatroyd (1969) and CIRA (1972) place the easterly maximum somewhat higher, at about 70 km and 60 km, respectively. (They differ widely, however, in the latitude of the easterly maximum—a fact that illustrates our relative ignorance of the climatology of the region.)

In the following section are presented the results of calculations similar to those of Simmons but with the modification that the jet maximum is located about 15 km above the stratopause. This seemingly minor change has important consequences for the scale of the disturbances generated by the instability. Two distinct modes of instability appear; one, associated with the easterly shear at the stratopause, has preferred scales and period similar to those of Simmons; the second mode, associated with the curvature of the jet, is of larger scale and has properties similar to those of the observed two-day wave.

3. A one-dimensional stability analysis

We consider quasi-geostrophic flow on a mid-latitude beta-plane, linearizing the equations of motion about a basic state of density $\rho(z)$ where z is a log-pressure height (e.g., Holton, 1979). The perturbation potential vorticity equation is

$$\left(\frac{\partial}{\partial t} + \bar{u}\frac{\partial}{\partial x}\right)q' + v'\frac{\partial \bar{q}}{\partial y} = -\frac{f^2}{\rho}\frac{\partial}{\partial z}\left(\frac{\rho\alpha}{N^2}\frac{\partial \psi'}{\partial z}\right), \tag{4}$$

where x and y are eastward and northward coordinates and α the Newtonian cooling rate; ψ' is the perturbation streamfunction, $v' = \partial\psi'/\partial x$ the northward perturbation velocity and

$$q' = \frac{\partial^2\psi'}{\partial x} + \frac{\partial^2\psi'}{\partial y^2} + \frac{f^2}{\rho}\frac{\partial}{\partial z}\left(\frac{\rho}{N^2}\frac{\partial \psi'}{\partial z}\right), \tag{5}$$

the perturbation potential vorticity. The basic state potential vorticity gradient is

$$\frac{\partial \bar{q}}{\partial y} = \beta - \frac{f^2}{\rho}\frac{d}{dz}\left(\frac{\rho}{N^2}\frac{d\bar{u}}{dz}\right). \tag{6}$$

Looking for solutions of the form

$$\psi'(x, y, z, t) = \mathrm{Re}\Psi(z)\, e^{ik(x-ct)} \sin ly, \tag{7}$$

Eq. (4) reduces to

$$(\bar{u} - c)\left[\frac{f^2}{\rho}\frac{d}{dz}\left(\frac{\rho}{N^2}\frac{d\Psi}{dz}\right) - (k^2 + l^2)\Psi\right] + \frac{\partial \bar{q}}{\partial y}\Psi = \frac{if^2}{k\rho}\frac{d}{dz}\left(\frac{\rho\alpha}{N^2}\frac{d\Psi}{dz}\right). \tag{8}$$

The eigenvalue problem thus posed is closed by boundary conditions which are taken to be zero vertical velocity on the upper and lower boundaries. From the thermodynamic equation this gives

$$(\bar{u} - c)\frac{d\Psi}{dz} - \frac{d\bar{u}}{dz}\Psi = \frac{i\alpha}{k}\frac{d\Psi}{dz} \tag{9}$$

on the boundaries $z = z_1, z_2$. These boundaries are artificially set at $z_1 = 30$ km, $z_2 = 108$ km. As will be seen, these are sufficiently far removed from the

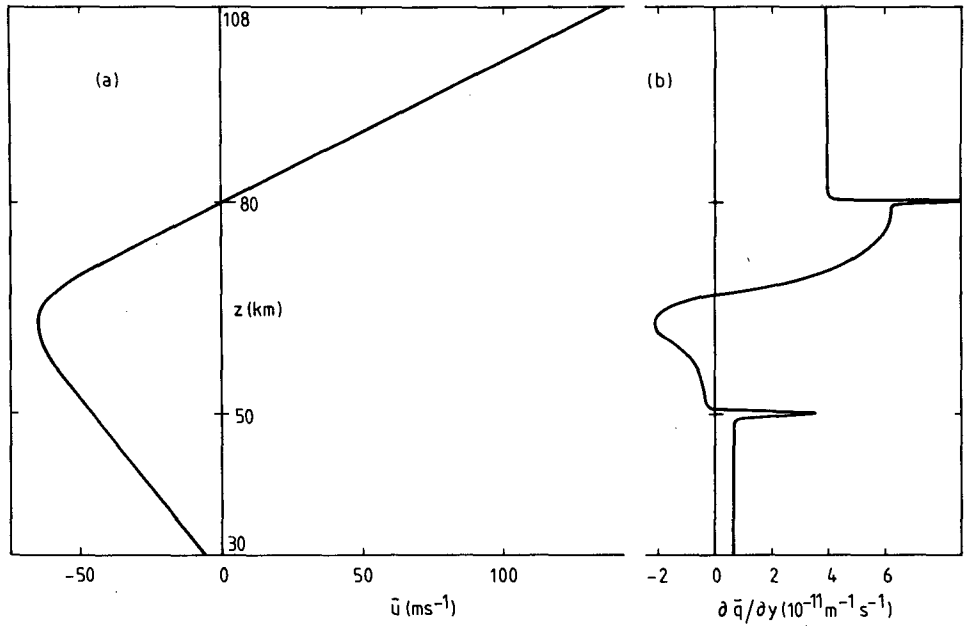

FIG. 1. The basic state as a function of height z for a flow with $\Lambda_1 = -2$ m s^{-1} km^{-1}, $\Lambda_2 = 5$ m s^{-1} km^{-1}: (a) mean zonal wind, (b) potential vorticity gradient.

source of instability in the mesosphere for their influence on the results to be negligible. The basic stratification is chosen such that $N^2 = 2.0 \times 10^{-4}$ s^{-2} within the mesosphere (50 km $< z <$ 80 km) and $N^2 = 4.0 \times 10^{-4}$ s^{-2} elsewhere. Density decays exponentially with scale height 7 km and the values $f = 1.0 \times 10^{-4}$ s^{-1} and $\beta = 1.6 \times 10^{-11}$ m^{-1} s^{-1} are adopted as representative of mid-latitudes. The meridional wavenumber l is π/L, where L is a suitable meridional length scale which is taken to be 5000 km, as representative of the jet width. The solution is obtained on a finite-difference grid of resolution 2 km.

The vertical wind structure is represented by a hyperbolic tangent shear

$$\frac{d\bar{u}}{dz} = \tfrac{1}{2}(\Lambda_1 + \Lambda_2) - \tfrac{1}{2}(\Lambda_1 - \Lambda_2)\tanh\left(\frac{z - z_0}{\delta}\right), \quad (10)$$

where, for most cases, $z_0 = 65$ km and $\delta = 5$ km. To fix the actual wind speed, the jet maximum was set at -65 m s^{-1} (but note that any constant may be added to $\bar{u}$ provided that the same constant is added to c).

The mean wind and potential vorticity gradient profiles for $\Lambda_1 = -2$ m s^{-1} km^{-1} and $\Lambda_2 = 5$ m s^{-1} km^{-1} are shown in Fig. 1. The uniform westerly shear at high levels produces unrealistically strong flow above 85 km or so but, as will be seen below, the dynamically important region, as evidenced by the distribution of EP flux and its divergence, lies within the mesosphere, and the high-level flow has negligible influence on the instability being investigated (cf. Simmons, 1977). This has been checked by setting $\bar{u}$ to a constant value above 85 km. The necessary condition for instability (Charney and Stern, 1962) is met with $\partial\bar{q}/\partial y$ being negative in the region of jet maximum and down to the stratopause. The negative peak in $\partial\bar{q}/\partial y$ is associated with the jet curvature; the weaker negative region below arises from the easterly shear. With $\rho(z) = \rho(0)\exp(-z/H)$, Eq. (6) may be written

$$\frac{\partial\bar{q}}{\partial y} = \beta - \frac{f^2}{N^2}\frac{d^2\bar{u}}{dz^2} + \frac{f^2}{N^2 H}\frac{d\bar{u}}{dz} - f^2\frac{d\bar{u}}{dz}\frac{d}{dz}\left(\frac{1}{N^2}\right). \quad (11)$$

From the third term on the right-hand side of (11), $\partial\bar{q}/\partial y$ will be negative in the absence of flow curvature and nonuniform stratification if the shear is strong and easterly, i.e., if

$$-\frac{d\bar{u}}{dz} > \frac{N^2}{f^2}\beta H = 2.24 \text{ m s}^{-1} \text{ km}^{-1} \quad (12)$$

(cf. Simmons, 1974) in the mesosphere. [The fact that $\partial\bar{q}/\partial y$ is negative in the lower mesosphere in Fig. 1b with shear slightly less than given by (12) is partly due to weak curvature and partly to finite difference error.] The localized, large positive contributions to $\partial\bar{q}/\partial y$ are associated with the discontinuities[1] in N^2.

Results of the stability analysis with $\alpha = 0$, shown in Fig. 2, confirm the instability of this profile in the absence of radiative dissipation. Two distinct modes of instability are found which, as will be seen, seem to be separately associated with the two zeros in $\partial\bar{q}/\partial y$. The more rapidly growing of these, which in

[1] Note that, in the finite difference equations, these discontinuities are in fact smoothed over one grid increment (2 km).

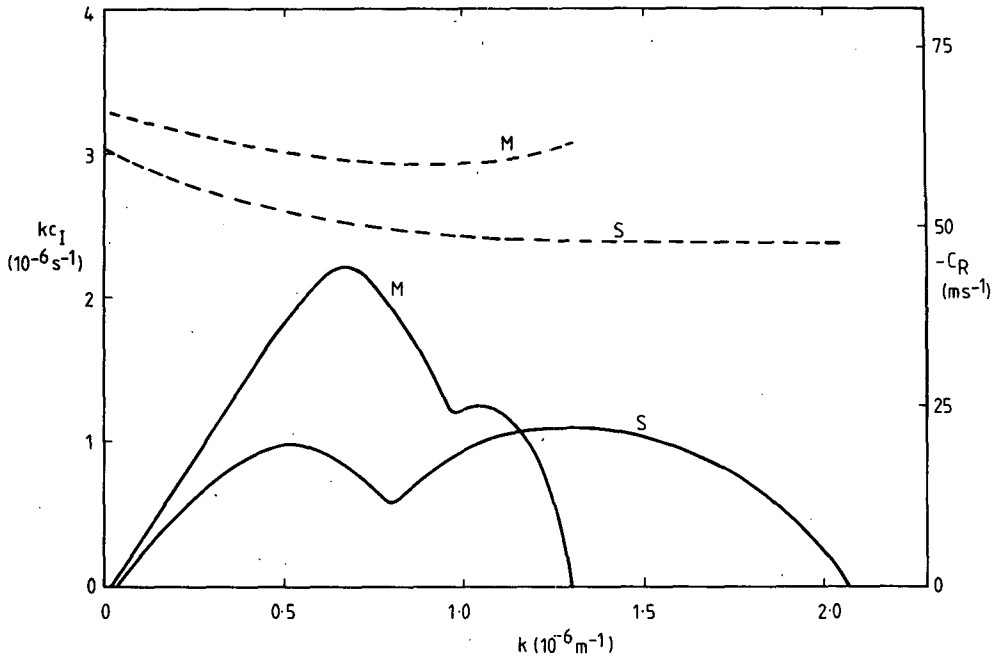

FIG. 2. Adiabatic growth rate kc_I (solid) and phase speed c_R (dashed) for the fastest growing wave perturbations to the flow of Fig. 1 as a function of zonal wavenumber k. M: mesospheric mode, S: stratopausal mode.

this case is the "mesospheric" mode associated with the upper zero, has a maximum growth rate of (5.21 days)$^{-1}$ at a zonal wavelength of 9300 km. The phase speed of this mode is, for all wavenumbers, about -60 m s^{-1}, a little slower than the maximum wind speed. The second "stratopausal" mode has maximum growth rate of (10.3 days)$^{-1}$ at a wavelength of 4800 km; its phase speed is somewhat slower, at about -48 m s^{-1}. The structure of the two modes for a zonal wavelength of 9400 km is shown in Figs. 3 and 4. For the mesospheric mode (Fig. 3), $|\Psi|$ has a maximum at the mesopause and a weak secondary maximum at the stratopause. The phase of Ψ, which is here defined as $-\arg(\Psi)$, shows a maximum in the lower mesosphere, a decrease of about one-quarter wavelength up to the mesopause, becoming almost independent of height above. Below the stratopause the structure is similarly almost barotropic. Note the weak increase of phase with height in the lowest 6 km or so of the mesosphere. The structure of $|\partial\Psi/\partial z|$ (which is, of course, proportional to temperature amplitude) shows a clear maximum in the region of the jet with a large secondary maximum at the mesopause and a much weaker one at the stratopause. To fix relative amplitudes, if we associate the peak in $|\Psi|$ at the mesopause with a northward velocity amplitude of 10 m s^{-1}, then the temperature maximum is 4.5 K at 67 km.

The structure of the stratopausal mode (Fig. 4) differs in a number of ways. There is again a mesopausal maximum in $|\Psi|$, but with a strong secondary maximum at the stratopause. A similar secondary peak, just below the stratopause, is evident in the temperature amplitude. The geopotential phase structure is similar to that of the mesospheric mode. The distinction between the two modes becomes apparent in the meridional heat flux,

$$\overline{v'T'} = \frac{fkH}{R}\,\mathrm{Im}\left(\Psi^* \frac{d\Psi}{dz}\right), \tag{13}$$

where R is the gas constant, and the vertical component of the EP flux,

$$F_z = \rho\,\frac{kf^2}{N^2}\,\mathrm{Im}\left(\Psi^* \frac{d\Psi}{dz}\right), \tag{14}$$

as shown in Figs. 3c and 4c. Both modes exhibit the properties predicted by (3) with extrema of F_z coinciding with zeros in the potential vorticity gradient, the upper maximum having upward EP flux (poleward eddy heat flux) with the opposite signs in the lower region. The difference between the two modes lies in the relative magnitudes of these two components. For the mesospheric mode the fluxes are dominated by the upper, positive region which is associated with the upper zero in $\partial\bar{q}/\partial y$ (and therefore, as noted above, the jet curvature) and the EP flux is predominantly directed from the lower to the upper mesosphere. The stratopausal mode, however, has regions of poleward heat flux around 70 km and equatorward heat flux in the lower mesosphere, both of comparable magnitude; the EP flux is dominated by the lower branch, downward from the lower mesosphere into the stratopause. Therefore, this mode

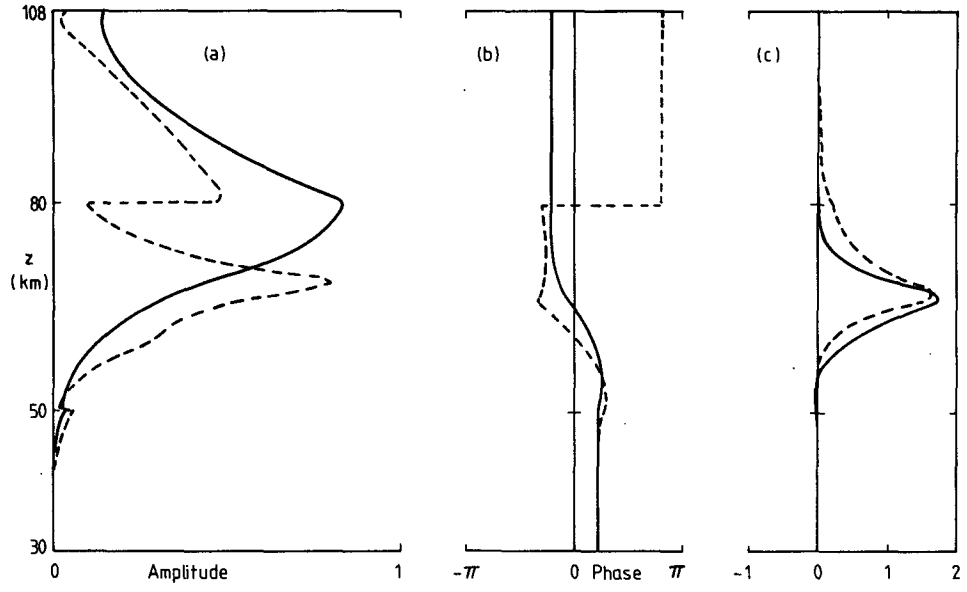

FIG. 3. Structure of the mesospheric mode as a function of height for the flow of Fig. 1 and a zonal wavelength of 9400 km. (a) Geopotential amplitude $|\Psi|$ (solid), "temperature" amplitude $|d\Psi/dz|$ (dashed). Amplitude scale is arbitrary, but see text for a discussion of relative amplitudes. (b) Phase of geopotential (solid) and temperature (dashed). (c) Heat flux $v'T'$ (dashed) and Eliassen-Palm flux (solid). Amplitude scale is arbitrary.

is apparently associated with the lower zero in $\partial\bar{q}/\partial y$ which in turn derives from the easterly shear at the stratopause.

Note the distinction, however, between this instability and that predicted as a possibility at the *winter* stratopause (Simmons, 1974). In the winter case negative values of $\partial\bar{q}/\partial y$ occur only at the stratopause itself; in (11) this occurs through the term involving $d(1/N^2)/dz$. In the summer case the stratopause is a boundary between the positive values of $\partial\bar{q}/\partial y$ in the upper stratosphere and negative values in the lower mesosphere. The stratopausal maximum in $\partial\bar{q}/\partial y$ plays a relatively minor role; indeed some experiments run with a more gradual change of stability at the stratopause showed that the growth rate of the stratopausal mode is not very sensitive to such variation.

From this and the many other cases studied it was

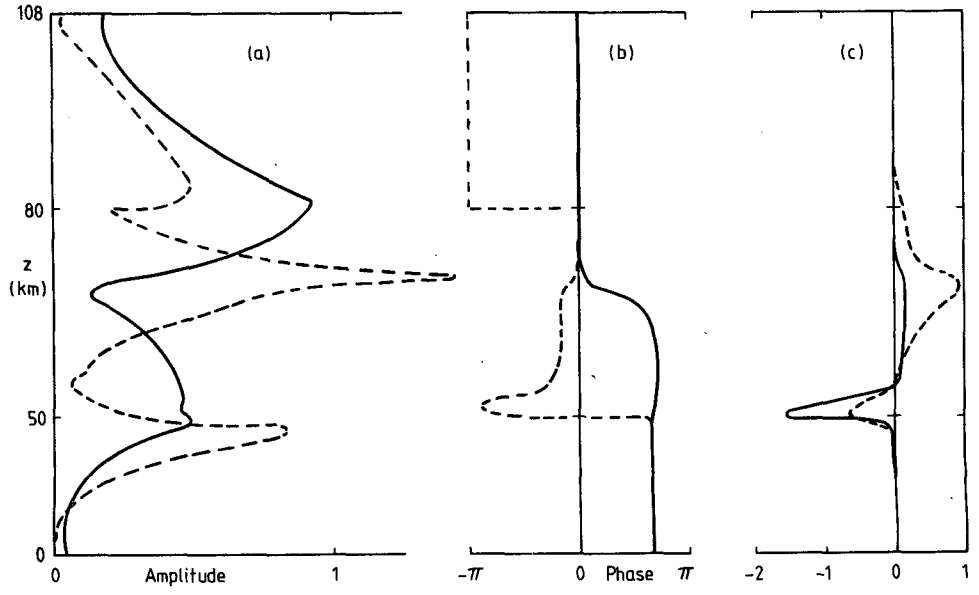

FIG. 4. As in Fig. 3 but for the stratopausal mode.

found that the phase speed of the mesospheric mode is in most cases about +4 m s^{-1}, relative to the easterly jet maximum, while that of the stratopausal mode is about −5 m s^{-1} (depending on k) relative to the wind at the stratopause. Therefore, relative to the ground, the phase speed of both modes is dominated by simple advection, as found by Simmons (1977).

The dependence of growth rates and wavelengths of the most rapidly growing waves on the lower and upper shears Λ_1 and Λ_2 is shown in Table 1. With fixed Λ_2, the growth rate of the stratopausal mode increases rapidly with increasing Λ_1 (Runs A, B, C, D). For the smaller values of Λ_1 the long-wave branch (cf. Fig. 2) dominates, but with $-\Lambda_1 \geq 2$ m s^{-1} maximum growth is found in the shorter waves. The growth rate and wavelength of the mesospheric mode are almost independent of Λ_1 in the range shown. For smaller values of Λ_2, the stratopausal mode disappears and the growth rate of the mesospheric mode decreases a little. With fixed Λ_1 and increasing Λ_2 the opposite behavior is found, with little change in the stratopausal mode but increasingly rapid growth and slowly increasing wavelength of the mesospheric mode. These results differ from those of Simmons (1977) in that, for those cases dominated by the mesospheric mode (all except C and D in Table 1), the zonal wavelength of maximum instability is in the range 8000–10000 km, about twice that found by Simmons (who took $l = 0$ and used basic states with jet maxima closer to the stratopause).

The time scale for wave growth in these adiabatic calculations may be less than 4 days for $\Lambda_2 \geq 6$ m s^{-1} km^{-1}, which is of the magnitude suggested by observations (e.g., CIRA, 1972; Hirota, 1975; R. A. Vincent, private communication, 1982). However, in the presence of realistic thermal dissipation, this growth will be greatly reduced. Blake and Lindzen (1973) give values of about 2 days for the timescale of radiative-photochemical damping in the lower mesosphere, although their result probably exaggerates the contribution of photochemical acceleration (Hartmann, 1978). Recent work by Fels (1982), however, gives a similar value of about (2 days)$^{-1}$ in this region for the scale-dependent damping rate of temperature perturbations with vertical wavelength of 12.6 km, which is reasonably representative of the temperature structure in these calculations (cf. Figs. 3 and 4).

Simmons (1977) found that for a constant value of α, the growth rates were reduced by about 0.5α, as compared with the adiabatic results. This was confirmed in the present results, as illustrated in Fig. 5. (Apart from the reduction in the growth rate, inclusion of nonzero α had relatively little effect on phase speeds or structure of the growing waves.) Therefore only those cases for which the adiabatic growth rate is greater than about (4 days)$^{-1}$ are likely in reality to generate instability. From Table 1, this apparently requires a stratospheric easterly shear of at least 3 m s^{-1} km^{-1} (which seems larger than "climatologies" suggest) or a westerly shear in the upper mesosphere in excess of 6 m s^{-1} km^{-1}. As noted earlier, this latter requirement may in fact be met in the summer mesosphere. Note that, by suppressing the weaker instabilities, the effects of damping will be to confine the instability to the peak of the growth rate curve.

Other cases were studied in which z_0 and δ, the altitude and width of the jet, respectively, were varied. Changing z_0 by ±5 km made a small difference to the features discussed above, without affecting the qualitative nature of the results. (Recall, however, the more dramatic effects of reducing z_0 by 15 km, when the mesospheric mode is suppressed altogether.) Decreasing δ, and hence increasing the jet curvature, made little difference to the stratopausal mode, but intensified the growth of the mesospheric mode. The value of 5 km used above gives what appears to be a reasonable jet curvature but our knowledge of the structure of this jet is insufficient to define this very precisely. Another factor that could intensify the instability is the barotropic curvature of the jet; the barotropic component of the potential vorticity gradient for representative jets is negative and almost as large as the baroclinic component. This aspect is beyond the scope of this one-dimensional analysis and will be addressed in a subsequent paper.

4. Discussion

For westerly upper mesospheric shear in excess of 6 m s^{-1} km^{-1}, these calculations indicate that the

TABLE 1. Growth times $T = (kc_i)^{-1}$ and zonal wavelength $\lambda = (2\pi k)^{-1}$ of the fastest growing waves as a function of low-level shear Λ_1 and high-level shear Λ_2.

			Stratopausal mode		Mesopheric mode	
	Λ_1 (m s^{-1} km^{-1})	Λ_2 (m s^{-1} km^{-1})	T (days)	λ (10^3 km)	T (days)	λ (10^3 km)
A	−1.5	4.0	10.5	9.3	6.36	8.4
B	−2.0	4.0	10.1	4.9	6.88	8.3
C	−2.5	4.0	5.71	5.4	6.38	7.2
D	−3.0	4.0	4.61	5.8	6.84	7.9
E	−2.0	5.0	10.3	4.8	5.21	9.3
F	−2.0	6.0	10.1	4.9	4.26	9.9
G	−2.0	7.0	10.1	4.6	3.68	9.9

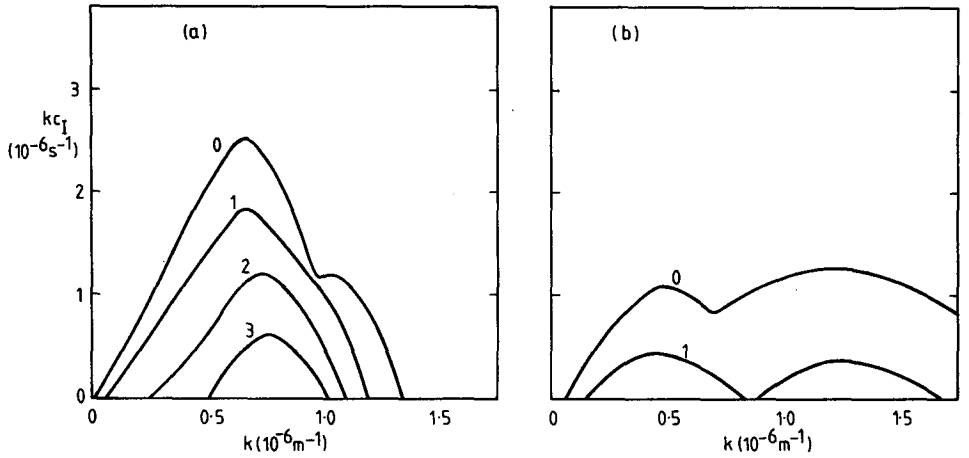

FIG. 5. Growth rate of the fastest growing wave perturbations to the flow of Fig. 1 as a function of zonal wavenumber and for a range of values of the thermal dissipation rate α; curves are labelled with values of α (10^{-6} s^{-1}). (a) Mesospheric mode, (b) stratopausal mode. The flow is stable for values of α greater than those shown.

mesospheric jet will be unstable, with the most rapidly growing wave having a zonal wavelength of ~10 000 km and a westward phase velocity of ~60 m s^{-1}. At middle latitudes, this corresponds to a zonal wavenumber of about 3 with a period around 2 days and it is tempting to associate this prediction with the observed quasi-two-day wave. Baroclinic growth may in fact occur for a range of wavenumbers, all with similar phase speeds, and it is interesting to note in this regard that observations indicate the presence in the summer mesosphere of a wave of wavenumber 4 and period about 1.7 days (Rodgers and Prata, 1981; Cevaloni *et al.*, 1981) which could also be a product of baroclinic instability.

With a strong easterly stratospheric shear, the stratopausal mode may become unstable also; in this case maximum growth occurs at zonal wavelengths ~ 5000 km and westward phase velocities of ~50 ms^{-1}, which correspond to zonal wavenumbers of 5–6 and periods around 1 day. These waves are similar to those predicted by Simmons (1977).

The wave periods are primarily determined by the strength of the jet. Therefore the apparent reproducibility of period of the two-day wave from one year to the next is consistent with an interpretation along these lines only if the jet is similarly reproducible; whether or not this is the case is difficult to establish. By the same token, the apparent difference in period between January and July would imply a corresponding difference in the jet velocities in the southern and northern summer mesospheres respectively.

There is very little basis for a detailed structural comparison between the observed two-day wave and the baroclinic waves described here. Certainly the decay with height of $|\Psi|$ above the mesopause is not well supported by observations and the satellite data suggest that the upper stratospheric temperature amplitudes are much larger, relative to amplitudes in the mesosphere, than these results suggest. Further, while the meridional heat fluxes agree in sign with the GCM results of Hunt (1981a,b), the magnitude of the equatorward heat fluxes for the mesospheric mode is extremely small. (In other respects it is the mesospheric rather than the stratopausal mode that most closely resembles Hunt's wave.) However, it should be noted that these linear results can only give a broad indication of the structure of the mature, finite-amplitude disturbance; it is well known, for example, that mature baroclinic disturbances in the troposphere are much more extensive in the vertical than linear models predict (e.g., Simmons and Hoskins, 1978). Obviously, this one-dimensional analysis gives no information as to latitudinal structure; solutions in a spherical model will be discussed in a subsequent paper.

This interpretation does give a simple explanation of the seasonality of the observed two-day wave. Around the solstices, the stratospheric easterlies in the summer hemisphere intensify as the high-latitude regions are heated. Almost simultaneously, a strong westerly shear develops in the upper mesosphere, probably driven by internal gravity wave radiation stresses (Lindzen, 1981; Holton, 1982; Matsuno, 1982). Eventually this shear may become so strong that the jet becomes baroclinically unstable, a process that could be manifested by the appearance of the two-day wave. The effect of the instability on the jet itself would probably be to limit the jet curvature and the intensity of this westerly shear. With the seasonal decay of the easterly jet in late summer, the flow will be stabilized and the two-day wave would then collapse.

This scenario is consistent with the seasonality reported by most observers as described in the Introduction. It is not, however, tenable if the wave is clearly identified around the equinoxes, and it re-

mains to be seen whether Salby and Roper's (1980) observation of a significant two-day wave in autumn is confirmed by future studies.

Another aspect of the two-day wave that appears to be central to this theory is the reversed phase structure (downward propagation) in the lower mesosphere. Although the amplitude of the linear mesospheric mode is extremely small in this region, that of the finite-amplitude disturbance may not be, as noted above, and indeed the satellite data indicate significant amplitude of the observed two-day wave at least down to the upper stratosphere. Note, however, that this phase behavior is a predicted property of the geopotential (or meridional velocity) perturbation; the phase structure of the temperature perturbation may differ from this (cf. Figs. 3 and 4). Wind measurements in the lower mesosphere are required to test this aspect of the predictions.

Acknowledgments. I am grateful to R. L. Craig, B. G. Hunt and R. A. Vincent for discussions on observational and modelling aspects of the two-day wave and for comments on an earlier draft of this paper.

REFERENCES

Aso, T., T. Tsuda, Y. Takashima, R. Ito and S. Kato, 1980: Observations of lower ionospheric wind by the Kyoto meteor radar. *J. Geophys. Res.*, **85,** 177–184.

Blake, D., and R. S. Lindzen, 1973: The effect of photochemical models on calculated equilibria and cooling rates in the stratosphere. *Mon. Wea. Rev.*, **101,** 783–802.

Cevaloni, G., S. P. Kingsley and H. G. Muller, 1981: Simultaneous observations of the quasi 2-day neutral wind oscillation in the meteor region over latitudes 45 to 60 degrees North. Presented at Middle Atmosphere Symposium, 4th IAGA Scientific Assembly, Edinburgh, 3–15 August 1981. [Abstracts published by IUGG Publications Office, Paris].

Charney, J. G., and M. E. Stern, 1962: On the stability of internal baroclinic jets in a rotating atmosphere. *J. Atmos. Sci.*, **19,** 159–172.

CIRA, 1972: *COSPAR International Reference Atmosphere.* Akademie-Verlag, Berlin.

Coy, L., 1979: A possible 2-day oscillation near the tropical stratopause. *J. Atmos. Sci.*, **36,** 1615–1618.

Craig, R. L., and W. G. Elford, 1981: Observation of the quasi two-day wave near 90 km altitude. *J. Atmos. Terr. Phys.*, **43,** 1051–1056.

——, R. A. Vincent, G. J. Fraser and M. J. Smith, 1980: The quasi-2-day wave in the Southern Hemisphere mesosphere. *Nature,* **287,** 319–320.

Dickinson, R. E., 1973: Baroclinic instability of an unbounded zonal shear flow in a compressible atmosphere. *J. Atmos. Sci.*, **30,** 1520–1527.

Edmon, H. J., B. J. Hoskins and M. E. McIntyre, 1980: Eliassen-Palm cross-sections for the troposphere. *J. Atmos. Sci.*, **37,** 2600–2616.

Fels, S. B., 1982: A parameterization of scale-dependent radiative damping rates in the atmosphere. *J. Atmos. Sci.*, **39,** 1141–1152.

Glass, M., J. L. Fellous, M. Massebeuf, A. Spizzichino, I. A. Lysenko and Yu. I. Portniaghin, 1975: Comparison and interpretation of the results of simultaneous wind measurements in the lower thermosphere at Garchy (France) and Obninsk (USSR) by meteor radar technique. *J. Atmos. Terr. Phys.*, **37,** 1077–1087.

Hartmann, D. L., 1978: A note concerning the effect of varying extinction on radiative photochemical relaxation. *J. Atmos. Sci.*, **35,** 1125–1130.

Hirota, I., 1975: Spectral analysis of planetary waves in the summer stratosphere and mesosphere. *J. Meteor. Soc. Japan,* **53,** 33–44.

Holton, J. R., 1979: *An Introduction to Dynamic Meteorology,* 2nd ed. Academic Press, 391 pp.

——, 1982: The role of gravity wave induced drag and diffusion in the momentum budget of the mesosphere. *J. Atmos. Sci.*, **39,** 791–799.

Hunt, B. G., 1981a: The maintenance of the zonal mean state of the upper atmosphere as represented in a three-dimensional general circulation model. *J. Atmos. Sci.*, **38,** 2172–2186.

——, 1981b: The 2-day wave in the middle atmosphere as simulated in a general circulation model extending from the surface to 100 km. *J. Atmos. Terr. Phys.*, **43,** 1143–1154.

Kal'chenko, B. V., 1979: Latitude and longitude features of the two-day disturbances of the drift of meteor trails. *Meteor. Res.*, **6,** 16–19 (In Russian).

——, and S. V. Bulgakov, 1973: Study of periodic components of wind velocity in the lower thermosphere above the equator. *Geomag. Aeronomy,* **13,** 955–956.

Kingsley, S. P., H. G. Muller, L. Nelson and A. Scholefield, 1978: Meteor winds over Sheffield (53°N, 2°W). *J. Atmos. Terr. Phys.*, **40,** 917–922.

Lindzen, R. S., 1981: Turbulence and stress due to gravity wave and tidal breakdown. *J. Geophys. Res.*, **86,** 9707–9714.

Matsuno, T., 1982: A quasi-one-dimensional model of the middle atmosphere circulation interacting with internal gravity waves. *J. Meteor. Soc. Japan,* **60,** 215–226.

McIntyre, M. E., 1972: Baroclinic instability of an idealized model of the polar-night jet. *Quart. J. Roy. Meteor. Soc.*, **98,** 165–174.

Muller, H. G., 1972: Long-period meteor wind oscillations. *Phil. Trans. Roy. Soc. London,* **A271,** 585–598.

——, and S. P. Kingsley, 1974: On the scale sizes of wind systems in the meteor zone. *J. Atmos. Terr. Phys.*, **36,** 1851–1861.

——, and L. Nelson, 1978: A travelling quasi 2-day wave in the meteor region. *J. Atmos. Terr. Phys.*, **40,** 761–766.

Murgatroyd, R., 1969: The structure and dynamics of the stratosphere. *The Global Circulation of the Atmosphere,* G. Corby, Ed., Roy. Meteor. Soc., 159–195.

Prata, A. J., and C. F. Rogers, 1981: A comparison of 5-day and 2-day travelling wave observations with Hough modes modified by meridional shear. *Handbook for MAP,* Vol. 2, S. K. Avery, Ed. [Available from SCOSTEP Secretaritat, University of Illinois].

Rodgers, C. D., and A. J. Prata, 1981: Evidence for a travelling 2-day wave in the middle atmosphere. *J. Geophys. Res.*, **86,** 9661–9664.

Salby, M. L., 1981: The 2-day wave in the middle atmosphere: observations and theory. *J. Geophys. Res.*, **86,** 9654–9660.

——, and R. G. Roper, 1980: Long-period oscillation in the meteor region. *J. Atmos. Sci.*, **37,** 237–244.

Simmons, A. J., 1974: Baroclinic instability at the winter stratopause. *Quart. J. Roy. Meteor. Soc.*, **100,** 531–540.

——, 1977: Baroclinic instability in the summer mesosphere. *Quart. J. Roy. Meteor. Soc.*, **103,** 211–215.

——, and B. J. Hoskins, 1978: The life cycles of some nonlinear baroclinic waves. *J. Atmos. Sci.*, **35,** 414–432.

Stening, R. J., C. E. Meek, A. H. Manson and D. G. Stephenson, 1978: Winds and wave motions to 110 km at mid-latitudes VI. Tidal, gravity and planetary waves, 1976. *J. Atmos. Sci.*, **35,** 2194–2204.